

Ghost in the Context: Measuring Policy-Carriage Failures in Decision-Time Assembly

Igor Santos-Grueiro
International University of La Rioja
Logroño, Spain

Abstract

LLM agents do not act on raw interaction history; they act on a bounded decision state assembled by truncation, summarization, reordering, and rewriting. If directive-bearing state is dropped, weakened, or rebound during that step, an agent can cross a policy boundary without prompt override, model changes, or persistent-memory compromise. We study this failure mode over local Llama 3.1 8B, Qwen 2.5 7B, and Mistral 7B using judged exact constraint respect and direct audits of assembled-state visibility.

We evaluate *SAFECONTEXT*, a control layer that pins control state, reuses retained control prefixes, and optionally injects reminders under pressure while keeping model weights fixed. Unmitigated risk is systematic, but absolute exact compliance remains low. Against truncation, *SAFECONTEXT* yields small gains; against a strong structured-compaction policy, most aggregate lift disappears, leaving residual benefit mainly in overflow eviction and selected aliasing slices. Replay-only does not explain the effect. A larger-model extension on Qwen 14B and Llama 70B shows the same failure object under larger models, although sign and magnitude remain policy-conditional. Decision-time context assembly is therefore a measurable part of the control path that can be partially hardened.

CCS Concepts

• **Security and privacy** → **Software and application security**; *Software security engineering*; Domain-specific security and privacy architectures.

Keywords

LLM security, context management

1 Introduction

LLM agents do not answer from raw interaction history. Before the final model call, an orchestration layer assembles a bounded decision-time context by truncating, summarizing, reordering, and rewriting prior state. We call that subsystem *decision-time context assembly*; the model-visible prompt it emits is the *decision state*.

Deployed stacks often run under a much smaller effective working budget than the backend context window would suggest. Tool outputs, planner notes, retrieved snippets, system scaffolding, latency targets, and cost controls all compete for the same decision-time prompt budget. The security issue is not only what policy appears somewhere in raw history, but what policy survives into the assembled state that drives the action. When directive-bearing spans compete for that budget with tool traces and user content, they function as control state for the final action. If they are dropped, weakened, or rebound before decision time, the system can cross a

policy boundary even when the model never receives a conflicting privileged instruction.

While prior work motivates this concern, it does not isolate it as the primary threat target. Prompt-injection research studies takeover of the visible prompt surface [14, 24, 27, 34, 36]. Memory-poisoning and memory-defense work focus on persistent stores and retrieval-time replay [4, 21, 29, 30, 37]. Long-context and memory-optimization work study utility retention under bounded budgets [1, 5, 7, 28, 31, 35], while adjacent security work such as *CompressionAttack* studies semantic distortion inside compaction paths [9]. We focus on decision-time context assembly as a point in the control path where policy can fail without prompt override or persistent-memory compromise.

An explanation is generic transformation quality: perhaps a stronger summary, or brief replay of the right constraints, already accounts for the effect. We test that alternative directly through matched comparisons, including replay-only and stronger compaction policies rather than truncation alone.

We measure aligned local Llama 8B, Qwen 7B, and Mistral 7B in a limited-budget regime where assembly policy materially affects action time. The taxonomy has three families: *eviction*, where directive-bearing state no longer survives into the assembled decision state; *aliasing*, where transformed state survives but no longer preserves the same operative boundary; and *binding instability*, where the surviving rule is rebound to the wrong actor, object, or condition. The strongest evidence lies in eviction and aliasing; binding instability is evaluated separately. The core endpoints are judged exact constraint respect and direct audits of visible decision-state preservation. *SAFECONTEXT* is the evaluated control layer: it applies semantic control pinning (SCP), cache-aware reuse of pinned control prefixes, and optional Invasive Context Engineering (ICE) reminder reinjection while keeping model weights fixed. We also report a larger-model extension on Qwen 14B and Llama 70B, where model scale is coupled with serving-stack heterogeneity.

Unmitigated risk is systematic, and post-mitigation exact respect remains low. Against truncation, *SAFECONTEXT* yields small positive gains at explicit cost. Against stronger structured compaction, much of the aggregate lift disappears, and the residual benefit concentrates in overflow eviction and selected aliasing slices. The agentic-trace evaluation and reconstructed decision-state case make the mechanism concrete, while the larger-model extension shows that larger models do not erase it even though sign and magnitude remain policy-conditional. Under contested working budgets, decision-time context assembly is measurable and only partially hardenable.

Contributions.

- We formulate decision-time context assembly as a measurable part of the control path in LLM agents, separate from

prompt-surface takeover and persistent-memory compromise.

- We operationalize a failure taxonomy centered on eviction and aliasing, and include binding instability as a third family.
- We measure those failures under matched multi-model comparisons using judged output-level endpoints plus direct decision-state audits, evaluate a control-layer intervention that keeps model weights fixed, and test the interpretation against replay-only and stronger structured-compaction policies.

The remainder of this paper is organized as follows. Section 2 defines decision-time context assembly, the threat model, and the failure taxonomy. Section 3 presents SAFECONTEXT, along with the evaluation metrics and experimental setup. Section 4 reports the empirical results. Section 5 discusses implications and limitations. Section 6 situates the paper in prior work. Section 7 concludes.

2 Background and Threat Model

2.1 Decision-Time Context Assembly

We model agent output as $a_t = M(E(H_t))$, where M is the base model and E is the subsystem that assembles bounded history into the final decision state before action time. The raw turn-local history H_t contains retained dialogue state, planner/tool state, directive-bearing candidates, and the final query. Admission inside E partitions that raw history into admitted control state S_{ctrl} and residual mutable state S_{data} ; the post-policy representation sent to the model is the decision state C_t .

The issue is not whether a directive appears somewhere in raw history, but whether it remains live and correctly bound in the decision state delivered to M . In that sense, E is part of the control path: it selects which state survives, transforms how that state is represented, and preserves or breaks the binding that makes a directive operative. The invariant is simple: control state must reach decision time live and correctly bound.

In deployed agent stacks, E is not a special module; it is the memory, truncation, summarization, thread-window, or planner-compaction logic that constructs the next prompt. We call *directive-bearing content* any span that constrains the final action, including allow/deny rules, confirmation requirements, authority constraints, and plan-selection rules.

Figure 1 shows the subsystem under study: directive-bearing and non-control state compete under pressure before action time.

2.2 The Adversarial Scheduler

The adversary controls scheduling pressure over visible interaction history: how much non-control content appears, where it appears, and how directive-bearing state is separated or framed. That pressure changes what survives truncation, how summaries rewrite earlier state, and whether bindings remain intact. The attack goal is simple: induce a policy-boundary violation at action time by breaking the control-state invariant inside E .

The defender holds model and runtime configuration fixed and applies the same orchestration policy to the reference and mitigated paths. Model weights, task logic, and hidden-system state are constant within matched comparisons. The attacker does not need

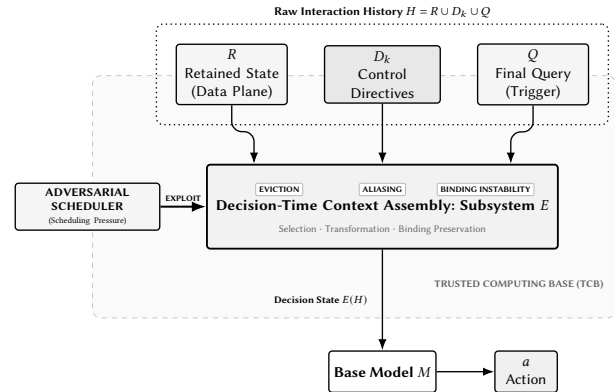


Figure 1: System and attack surface for $a = M(E(H))$. The relevant control boundary is not only the base model M , but also subsystem E , which decides which directives remain live in the decision state. Scheduling pressure on E is sufficient to induce eviction, aliasing, or binding instability before the decision state reaches the model.

jailbreak strings, privileged prompt override, persistent-store compromise, model-weight access, or hidden channels; visible-history scheduling pressure is sufficient. This isolates decision-time context assembly rather than prompt-surface takeover, persistent-memory poisoning, or generic long-context degradation. The same mechanism also appears without an active adversary: long tool outputs, planner notes, and routine conversational churn can impose the same pressure on earlier control state.

2.3 Failure Families

We organize the failure space around one question: after history passes through subsystem E , how can a directive stop governing the final action? It can disappear, survive in the wrong semantic form, or remain visible while governing the wrong object.

The three families are:

- (1) **Eviction:** the directive is displaced and no longer reaches decision time.
- (2) **Aliasing:** the directive survives, but only in a semantically weakened or rewritten form.
- (3) **Binding instability:** the directive remains visible, but the object it governs changes.

These families are defined operationally at the level of the decision state: eviction is a retention failure, aliasing a preservation-equivalence failure, and binding instability a binding failure.

A scenario belongs to a family only if the intended failure mode is identifiable in the decision state: absent directive for eviction, non-equivalent preserved directive for aliasing, and preserved directive with a changed referent for binding instability.

Here, a preserved directive is *operationally equivalent* to the original only if it induces the same admissible-versus-forbidden action boundary in the scenario under test. A paraphrase can remain equivalent; a softened summary or incomplete restatement cannot if it widens that boundary. Likewise, a *binding* is preserved only

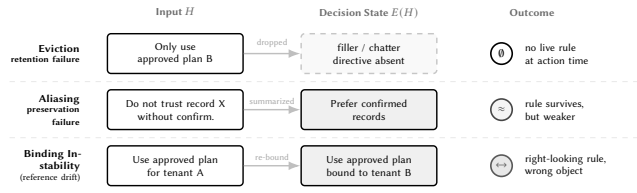


Figure 2: Failure traces from input history to decision state and outcome. Eviction removes the live directive, aliasing preserves only a non-equivalent rule-like trace, and binding instability preserves the rule text while rebinding it to the wrong object.

if the directive still governs the same object, record, plan, or tool output as in the original interaction.

This taxonomy is anchored in decision-state artifacts rather than surface textual similarity. The operative question is whether the rule that reaches answer time preserves the same action boundary as before transformation.

Eviction (Availability Failure)

Eviction scenarios place directive-bearing content early enough in the dialogue for finite-window pressure to remove it before answer time. Pressure and ordering are sufficient. At answer time, the directive is absent from the assembled state: the model sees task-supporting content and the final query, but not the governing rule. Eviction is therefore a carriage failure by absence rather than reinterpretation.

Aliasing (Integrity Failure)

Aliasing scenarios keep the directive semantically relevant but force it through compaction. The directive does not vanish; it survives in distorted, partial, or weakened form. Aliasing therefore tests policy *integrity* rather than mere policy *presence*: a recap can remain rule-like while still widening the admissible action boundary.

Binding Instability

Binding instability extends the framework beyond dropping and compaction. Here the directive remains visible, but the referent it governs changes by the time the model answers. The rule text survives, but its actor, object, or condition no longer matches the original directive. It is the weakest family empirically, but it remains conceptually useful because policy carriage is not just token survival.

For eviction, the dominant signal is loss of directive carriage; for aliasing, preservation quality matters more than simple presence/absence; and for binding instability, the audit must be binding-sensitive. The metric mix therefore differs across families: direct visibility matters most for eviction, operational equivalence for aliasing, and binding-sensitive auditing for binding instability. In this paper, eviction and aliasing carry the evidentiary weight because they produce the clearest and most repeatable signal in the aligned matrix.

Algorithm 1: SAFECONTEXT per-turn assembly policy

Input : Raw history H_t ; reference policy E_0 ; budget B_t ; admission mode A ; SHL reference h ; trigger fraction τ

Output : Decision state C_t ; audit α_t ; telemetry ω_t

- 1 $S_{ctrl}, S_{data}, Q_t \leftarrow \text{ADMITCONTROL}(H_t, A)$
 - 2 $(B_{ctrl}, B_{data}) \leftarrow \text{BUDGETSPLIT}(B_t, S_{ctrl})$; $C_{pin} \leftarrow \text{PINCONTROL}(S_{ctrl}, B_{ctrl})$
 - 3 $C_{data} \leftarrow E_0(S_{data}, B_{data})$
 - 4 $\hat{k}_t \leftarrow \text{ESTIMATEPRESSURE}(C_{pin}, C_{data})$
 - 5 **if** $\hat{k}_t \geq \tau h$ **then**
 - 6 $(C_{pin}, C_{data}) \leftarrow \text{APPLYICE}(C_{pin}, C_{data})$
 - 7 $C_t \leftarrow \text{COMPOSE}(C_{pin}, C_{data}, Q_t)$
 - 8 $\alpha_t \leftarrow \text{ABSAUDIT}(C_t)$; $\omega_t \leftarrow \text{EMITTELEMETRY}(A, B_{ctrl}, B_{data}, \hat{k}_t, \tau, h)$
 - 9 **return** $(C_t, \alpha_t, \omega_t)$
-

3 SAFECONTEXT Control-Layer Design

SAFECONTEXT is the evaluated control layer for decision-time context assembly. Directive-bearing state should not compete with ordinary context in an unmanaged token budget. SAFECONTEXT therefore makes control-state handling explicit through admission, persistence, reinforcement, and audit, without changing model weights.

3.1 SAFECONTEXT Design

Core design. In SAFECONTEXT, directive-bearing state is admitted before budget competition and then protected by a reserved control budget. Cache-aware variants reuse the retained control prefix across turns instead of fully reserializing it, Invasive Context Engineering (ICE) re-injects short control reminders near the final query under pressure, and Authority Binding Score (ABS) audits whether surviving directives still bind to the intended objects.

At each turn, the policy layer maps raw history and a token budget into the decision state plus lightweight telemetry. The practical design invariants are straightforward: mediate control state before budget competition, give it an explicit budget floor, trigger reinforcement only under pressure, preserve stable bindings through transformation, and log enough telemetry to inspect failures after the fact. In autonomous mode, false negatives in admission can still reduce real control coverage, which is why routing-mode behavior is reported explicitly in C3/C4. Eviction stresses isolation; aliasing stresses preservation and recovery; binding instability stresses audit.

The per-turn pipeline is deterministic: classify incoming segments, isolate directive-bearing content, apply the reference context policy to the remaining data state, trigger reinforcement only when observed pressure reaches the configured SHL risk point, and audit binding integrity before final inference. Algorithm 1 makes that path explicit. BUDGETSPLIT enforces a control-state floor, APPLYICE injects bounded reminder lines over directive-bearing spans before composition, and ABSAUDIT checks actor/action/object/condition-polarity consistency in the assembled decision state. The structural path is linear in turn-local history size; C4 reports the empirical cost profile.

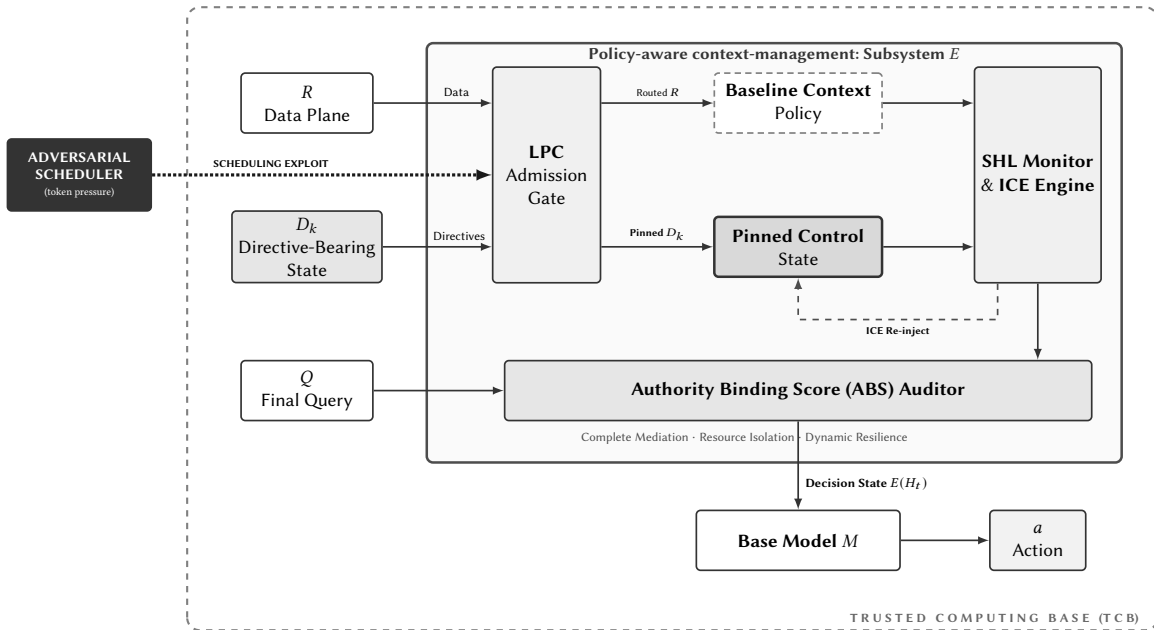


Figure 3: Control-layer intervention for decision-time context assembly: directive-bearing state is explicitly mediated before inference.

3.2 Admission Control: Lightweight Policy Classifier (LPC)

The first primitive is admission control. Incoming segments are tagged as POLICY or DATA before token-budget competition. In oracle mode, tags come from scenario-labeled directive spans; in autonomous mode, they are emitted by a lightweight LPC path complemented by prompt markers and simple control-language heuristics. This is a routing filter for control-bearing state, not a semantic oracle. Autonomous routing is the deployed path in the measured matrix; oracle routing isolates admission from the rest of the pipeline.

3.3 Deterministic Persistence: Cache-Aware Prefix Reuse

The second primitive is deterministic persistence. Directive-bearing segments are pinned into a protected control budget and, in cache-aware variants, the retained control prefix is reused across turns without being fully reserialized. Under scheduling pressure, data-plane expansion can consume the residual budget but cannot freely evict already pinned control state. SCP and SCP+Cache families are directly measured in the final matrix.

3.4 Active Resilience: SHL-Triggered ICE

The third primitive is active resilience. SHL (Security Half-Life) is measured in input-token pressure units: for a matched pressure-response curve, it is the smallest observed pressure level at which mean CSR falls below 0.5. Smaller SHL indicates earlier control-carriage collapse. ICE triggers when observed pressure reaches a configured fraction of a reference SHL estimate; if no reference

estimate is available, the implementation falls back to a context-window proxy. ICE therefore reinforces already admitted control state rather than replacing admission or pinning.

3.5 Integrity Verification: ABS Auditor

The output includes an integrity audit channel based on Authority Binding Score (ABS). The auditor checks whether directive bindings remain consistent after context transformation. ABS is an operational, judge-driven integrity check over actor/action/object/condition consistency in the assembled decision state. It covers the failure mode where rule text survives but authority pointers drift. The evaluated implementation therefore covers admission routing, persistence, SHL-triggered reinforcement, and ABS auditing at the orchestration layer.

3.6 Evaluation Metrics

We report four metric families. ECR asks whether the final answer exactly respects all applicable constraints. CSR measures partial respect. DFR asks whether changing only prompt order flips the judged control outcome in matched attack/control-last pairs. DPR audits the assembled decision state directly by measuring how many applicable constraints remain explicitly visible before the model call.

All comparisons are matched by *slice*: the task-level control condition is fixed and only the surrounding history or context treatment changes. This isolates assembly effects rather than generic prompt sensitivity.

3.7 Metric Definitions

Exact Constraint Retention Rate (ECR). ECR is an output-level exact-respect metric. For an instance i with a_i applicable constraints and r_i judged respected constraints, define the exact-respect indicator

$$\text{ecr}_i = \mathbf{1}[r_i = a_i].$$

For a slice S , ECR is the mean of these per-instance indicators:

$$\text{ECR}(S) = \frac{1}{|S|} \sum_{i \in S} \text{ecr}_i.$$

We report ΔECR between matched reference and mitigation slices. ECR asks whether the final answer remained on the governed side of the scenario boundary for the full applicable constraint set.

Decision Flip Rate (DFR). DFR is defined over matched order-perturbation pairs that keep semantic content fixed while changing only prompt order. For a paired scenario j , let v_j^{attack} and $v_j^{\text{control-last}}$ be binary judged violation outcomes under the two orderings. The pair contributes a flip iff these outcomes differ. For a slice with pair set P ,

$$\text{DFR}(S) = \frac{1}{|P|} \sum_{j \in P} \mathbf{1}[v_j^{\text{attack}} \neq v_j^{\text{control-last}}].$$

DFR is a paired instability metric that asks whether changing order alone changes the judged control outcome. Its natural unit is the matched pair.

Constraint Survival Rate (CSR). CSR is a graded secondary output-level metric for the question “how much of the governing rule is still respected at the final answer, even when exact preservation fails?” For an instance i with a_i applicable constraints and r_i judged respected constraints, the per-instance respect score is

$$\text{csr}_i = \frac{r_i}{\max(1, a_i)}.$$

For a slice S , CSR is the mean of these per-instance scores:

$$\text{CSR}(S) = \frac{1}{|S|} \sum_{i \in S} \text{csr}_i.$$

We report ΔCSR alongside ΔECR . Here, *constraint respect* means that the final answer remains on the side of the scenario’s control boundary intended by the original directive. CSR is therefore an output-level metric rather than a direct readout of what text or anchors remained present in the assembled decision state.

Direct Preservation Rate (DPR). To separate judged outcome from direct state visibility, we also audit the assembled decision state before the model call. For an instance i with a_i applicable constraints and p_i applicable constraints directly visible in the assembled decision state, define

$$\text{dpr}_i = \frac{p_i}{\max(1, a_i)}.$$

For a slice S , DPR is the mean of these per-instance visibility scores. A constraint counts as directly preserved when the assembled model-visible context still contains its explicit marker/text pair or the corresponding typed anchor. DPR is a direct visibility audit of the assembled decision state, not a semantic-equivalence metric: aliasing can leave directive-like text visible while still weakening the operative control boundary.

Judge scope and state-level scope. The evaluation pipeline uses automated judging to map model outputs into bounded control labels for ECR, CSR, and DFR. Concretely, it labels prohibited disclosure, deletion, external-tool use, or condition-bypass commitments, with explicit refusals and preserved gating conditions taking precedence over mere mention of the prohibited action. It acts as a bounded control-boundary classifier, not a general semantic grader.

ECR and CSR measure judged behavior at the output boundary, DFR measures paired order sensitivity, and DPR measures direct visibility in the assembled decision state before the model call. The submission package also includes an adjudicated manual subset over the main slices; on that task, agreement with the current judge is 52/60 with $\kappa = 0.73$.

Pressure and binding diagnostics. ABS and SHL diagnose binding integrity and pressure response. ABS is an operational audit over expected authority bindings in the assembled decision state and is used mainly for binding instability. SHL (Security Half-Life) is a pressure diagnostic measured in input-token pressure units: for a matched pressure-response curve, it is the smallest observed pressure level at which mean CSR drops below 0.5. Smaller SHL means earlier control-carriage collapse under pressure. In the implementation, ICE triggers when observed pressure reaches a configured fraction of a reference SHL estimate, with a context-window proxy used only when no SHL reference is available.

Uncertainty and what the metrics justify. For ECR, CSR, and DPR, we report slice-level bootstrap confidence intervals over per-instance scores, resampling instances within each slice. DFR is reported over matched order-perturbation pairs, ABS over bound-authority tuples, and SHL as a threshold estimate on the observed pressure grid.

Positive ΔECR together with positive ΔCSR indicates improved judged policy carriage in a given slice. Positive ΔDPR indicates that more applicable constraints remained directly visible in the assembled decision state, and negative ΔDFR indicates reduced order sensitivity. These metrics justify slice-level movement under matched conditions, not universal model behavior or a fully validated semantic oracle.

The design controls seed, scenario family, policy, mitigation state, and model configuration in the reported slices. It does not eliminate all heterogeneity in serving stack or all prompt-surface effects outside those comparisons.

3.8 Implementation and Experimental Setup

This section defines the evaluated implementation and the aligned closed campaign.

3.8.1 SAFECONTEXT Evaluated Implementation. We implement SAFECONTEXT as a middleware layer that perturbs decision-time context assembly without changing model weights. The evaluated implementation exposes four concrete controls: admission before budget competition, protected retention for directive-bearing state, cache-aware reuse of retained control prefixes, and pressure-triggered Invasive Context Engineering (ICE) reminders when control state starts to decay. At each turn, the middleware intercepts local history before the model call, normalizes it into typed segments, applies admission and context transformation, and emits

a hardened decision state while leaving the base model endpoint unchanged. The implementation targets OpenAI-compatible chat endpoints so the same logic can be reused across local serving stacks in this campaign. Here, “cache” denotes deterministic reuse of previously retained control prefixes at the orchestration layer rather than hardware-level KV pinning. Per-turn stage telemetry contextualizes C4 as an orchestration cost profile.

3.9 Methodology and Campaign Construction

The main quantitative analysis uses a single closed campaign over aligned local models and a fixed mitigation grid.

Campaign scope. The closed matrix spans:

- models: Llama 3.1 8B, Qwen 2.5 7B, Mistral 7B (aligned local setup),
- attacks: eviction, aliasing, and binding instability,
- seeds: 7, 11, 19,
- conditions: one unmitigated arm plus eight mitigation variants.

The mitigation variants are semantic control pinning (SCP), SCP+ICE, SCP+Cache, and SCP+Cache+ICE in oracle/autonomous modes where applicable. This yields a fixed target of 243 deduplicated cells. Within that matrix, eviction and aliasing carry most of the signal, while binding instability is smaller and noisier.

Larger-model extension. Beyond the closed 243-cell matrix, we evaluate two larger in-family models: Qwen 2.5 14B and Llama 3.1 70B. This extension reuses the same attack families, seeds, and mitigation grid, but runs on remote OpenAI-compatible backends, so model scale is entangled with serving-stack heterogeneity.

Run parameters (reproducibility-critical). The campaign uses fixed random seeds (7/11/19), fixed prompt-template families per attack class, and a fixed token-pressure bin grid used to estimate SHL on matched slices in input-token-pressure units. We evaluate frozen off-the-shelf instruct checkpoints rather than tuning model weights. In the aligned core, all three models are run under matched decoding settings with a 260-token context budget, a 96-token generation cap, and temperature 0.0. Prompt templates and scenario instantiations are versioned in the artifact bundle and referenced by the freeze manifest, which also identifies the model/runtime and policy configuration.

Why this budget regime. The relevant unit here is the *decision-time assembly budget*, not the advertised backend context window. The 260-token setting is deliberately severe but not arbitrary: small enough that policy competition becomes directly observable, yet still large enough to force realistic trade-offs among system scaffolding, tool traces, summaries, planner state, and the final query. This is the regime under study: a model-visible working budget that is much smaller than the raw backend window because orchestration overhead has already consumed the slack. The goal is not to numerically approximate every deployed stack or trace a monotonic law as budgets grow. The goal is to isolate a regime where the effective model-visible budget is genuinely contested, making context assembly part of the control path rather than neutral plumbing.

A 260-token decision state is not equivalent to a 260-token user prompt. In the traces studied here, that same budget must hold system scaffolding, retained control state, summaries or planner notes, retrieved snippets or tool outputs, and the final query. The reconstructed agentic case in Table 6 and Figure 6 makes this concrete: even short retrieved snippets and execution logs can consume most of the decision state before the final query arrives. The regime models an orchestration-constrained working prompt, not a bare model window with no surrounding state.

Scenario and prompt construction. Each scenario instance is generated from a structured template with five fields: control constraints, filler text, token budget, final query, and prompt order. Together, these fields preserve the directive-bearing policy boundary, inject benign pressure, keep task intent fixed, and create paired attack/control-last conditions for DFR analysis.

Policy behavior under test. The aligned core uses three reference assembly policies: B1 hard truncation, B2 rolling summary, and B3 hybrid. C2 adds a stronger competing policy, B2+, *strong structured compaction*; the same B2+ policy is reused in the matched agentic-trace evaluation. Mitigation variants apply admission, pinning, cache-assisted persistence, and reinforcement on top of those reference policies while holding model and task semantics fixed.

Token accounting for C4. The cost analysis counts model-visible input tokens plus emitted output or reinforcement tokens under the same orchestration-level accounting rule for every row. Cache-aware variants can therefore reduce total measured tokens relative to the unmitigated arm because pinned control segments are reused instead of being repeatedly reserialized into the assembled prompt. No row receives hidden backend-KV credit: serialized text is counted, reused retained segments are not counted again. All operating points are therefore compared at the same model-visible accounting boundary.

For a concrete accounting example, suppose a 40-token control segment must remain live across 10 turns. A non-cache policy that reserializes it each turn pays roughly 400 prompt tokens for that segment alone. A cache-aware path pays the initial serialization but not the repeated copies, so later turns are charged only for newly materialized summary, data, or reinforcement text. Negative token deltas in C4 therefore reflect avoided reserialization inside the harness, not unbilled backend reuse.

Mitigation families under test. The evaluated families are none (unmitigated), semantic control pinning (SCP), SCP+ICE, SCP+Cache, and SCP+Cache+ICE. We report both oracle and autonomous routing where available.

Data governance and freeze. We build a deduplicated per-cell master table and require full matrix completion before analysis. The final matrix reaches 243/243 cells. Final tables and figures are generated from this matrix only, and all reported artifacts are hash-traced in the submission bundle.

Implementation boundary and reproducibility. In oracle mode, SCP receives scenario-labeled directive spans and their retained representations inside the policy layer. This isolates routing from the rest of the pipeline and helps localize where control state is lost. Autonomous mode replaces those labels with the LPC path used

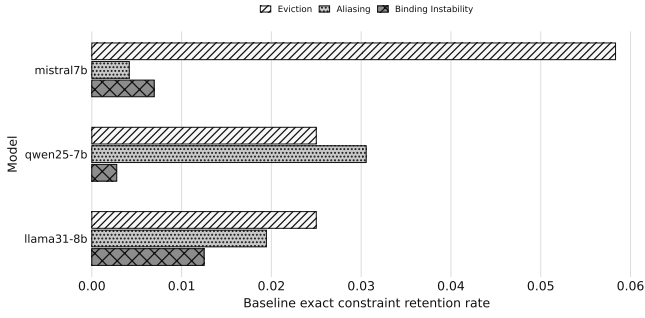


Figure 4: C1 unmitigated risk profile by model and attack family. Bars report unmitigated ECR for eviction, aliasing, and binding instability.

in the deployed comparisons. In deployment, the same principle could be instantiated through explicit metadata, prompt markers, tool-policy tags, safety-policy segments, or a lightweight directive recognizer.

4 Results

We organize the results around four questions: whether unmitigated risk is systematic (C1), whether preserving directive-bearing state still helps once stronger competing policies are considered (C2), whether the effect recurs across the aligned matrix (C3), and what cost it imposes (C4). ECR is the main judged metric, CSR the graded companion metric, DFR the paired order-sensitivity metric, and DPR the direct visibility audit of the assembled decision state.

C1: Unmitigated Risk Is Systematic

The unmitigated path already shows policy-carriage risk. Figure 4 shows unmitigated ECR by model and attack family. Judged exact respect is low across aligned models and families. Under bounded-budget competition, directive-bearing spans and ordinary history share the same prompt budget, so context growth can displace or weaken control state before answer time. The clearest signal appears in eviction and aliasing; binding instability is smaller and noisier. A frozen Llama 8B order-only run on overflow slices places the same directives last rather than under attack order and yields CSR in the 0.64–0.97 range, versus 0.36–0.50 under attack order. The task is therefore not uniformly unsatisfiable even in this low-budget regime.

C2: The Residual Effect Survives Only Against Stronger Competing Policies

C2 hinges on strong structured compaction (B2+); truncation alone is too weak a competing policy. In the aligned 7–8B core, we reran the unmitigated arm, SCP (A), and SCP+ICE (A) across aliasing and eviction. Table 1 shows the aggregate result. Against B2+, much of the aggregate gain disappears. Averaged across the full comparison, SCP (A) is slightly negative on ECR ($\Delta\text{ECR} = -0.012$) with $\Delta\text{CSR} = +0.029$; SCP+ICE (A) is effectively flat on ECR (-0.001) with $\Delta\text{CSR} = +0.059$. The slice-bootstrap ECR intervals cover zero for both overall rows.

Table 1: Strong structured-compaction policy (B2+). Values report residual gain over structured compaction itself, with 95% bootstrap CI over matched slices and both ΔECR and ΔCSR .

| Scope | Arm | Slices | ΔECR [95% CI] | ΔCSR [95% CI] |
|--------------------------|-------------|--------|-----------------------------|-----------------------------|
| Overall | SCP (A) | 9 | -0.012 [-0.038, 0.010] | 0.029 [0.009, 0.054] |
| Overall | SCP+ICE (A) | 9 | -0.001 [-0.017, 0.015] | 0.059 [0.029, 0.088] |
| Aliasing | SCP (A) | 3 | -0.003 [-0.009, 0.000] | 0.016 [-0.013, 0.032] |
| Aliasing | SCP+ICE (A) | 3 | 0.000 [-0.010, 0.015] | 0.072 [0.019, 0.111] |
| Aliasing (Qwen) | SCP (A) | 1 | 0.000 [0.000, 0.000] | 0.032 [0.032, 0.032] |
| Aliasing (Qwen) | SCP+ICE (A) | 1 | 0.015 [0.015, 0.015] | 0.111 [0.111, 0.111] |
| Aliasing (Llama+Mistral) | SCP (A) | 2 | -0.005 [-0.009, -0.001] | 0.008 [-0.013, 0.028] |
| Aliasing (Llama+Mistral) | SCP+ICE (A) | 2 | -0.007 [-0.010, -0.005] | 0.053 [0.019, 0.088] |
| Eviction | SCP (A) | 6 | -0.016 [-0.054, 0.016] | 0.036 [0.008, 0.067] |
| Eviction | SCP+ICE (A) | 6 | -0.002 [-0.026, 0.023] | 0.053 [0.017, 0.092] |
| Eviction (overflow) | SCP (A) | 3 | 0.007 [-0.009, 0.036] | 0.062 [0.015, 0.101] |
| Eviction (overflow) | SCP+ICE (A) | 3 | 0.008 [-0.008, 0.034] | 0.064 [0.054, 0.075] |
| Eviction (no overflow) | SCP (A) | 3 | -0.039 [-0.097, 0.021] | 0.010 [-0.002, 0.028] |
| Eviction (no overflow) | SCP+ICE (A) | 3 | -0.012 [-0.042, 0.039] | 0.041 [-0.011, 0.127] |

Table 2: Residual picture after strong structured compaction for the strongest deployable path, SCP+ICE (A). The surviving advantage is local rather than global.

| Scope | ΔECR [95% CI] | Reading |
|--------------------------|-----------------------------|---|
| Overall | -0.001 [-0.017, 0.015] | Flat overall once compaction is already strong. |
| Eviction (overflow) | +0.008 [-0.008, 0.034] | Small residual advantage where pressure is highest. |
| Eviction (no overflow) | -0.012 [-0.042, 0.039] | No stable residual benefit without overflow pressure. |
| Aliasing (Qwen) | +0.015 [0.015, 0.015] | Small positive residual in one concentrated slice. |
| Aliasing (Llama+Mistral) | -0.007 [-0.010, -0.005] | Flat to negative outside that concentrated slice. |

Single-slice rows yield degenerate bootstrap intervals by construction; they should be read as exact slice values, not as evidence of high precision. The residual signal is small and heterogeneous, concentrated mainly in pressure-heavy eviction and a few aliasing slices. Eviction-overflow rows stay slightly positive on ECR (+0.007 for SCP and +0.008 for SCP+ICE), whereas eviction without overflow turns flat-to-negative (-0.039 and -0.012). Once compaction is already strong, preserving directive-bearing state helps mainly where control-bearing state is under the most pressure.

Against matched truncation, the same intervention family still moves in a favorable direction. Figure 5 reports paired $\Delta\text{ECR}/\Delta\text{DFR}$ by family, and Table 3 ranks variants with 95% bootstrap CI and ΔCSR shown alongside ΔECR . The top rows remain positive on ECR, with the strongest mean lift in the low-hundredths. Absolute judged exact respect, however, remains low: averaged over the eviction+aliasing core cells, mean ECR rises from about 0.027 in the unmitigated arm to about 0.061 for SCP+ICE (A) and 0.067 for SCP+Cache+ICE (A). The truncation comparison therefore shows partial hardening, not high post-mitigation reliability. Autonomous rows are the deployed comparison; oracle rows isolate how much of the effect comes from routing.

Recency versus governance. To separate simple recency boosting from control-state governance, we ran a focused ablation on the aligned 7–8B triplet across aliasing and eviction with matched

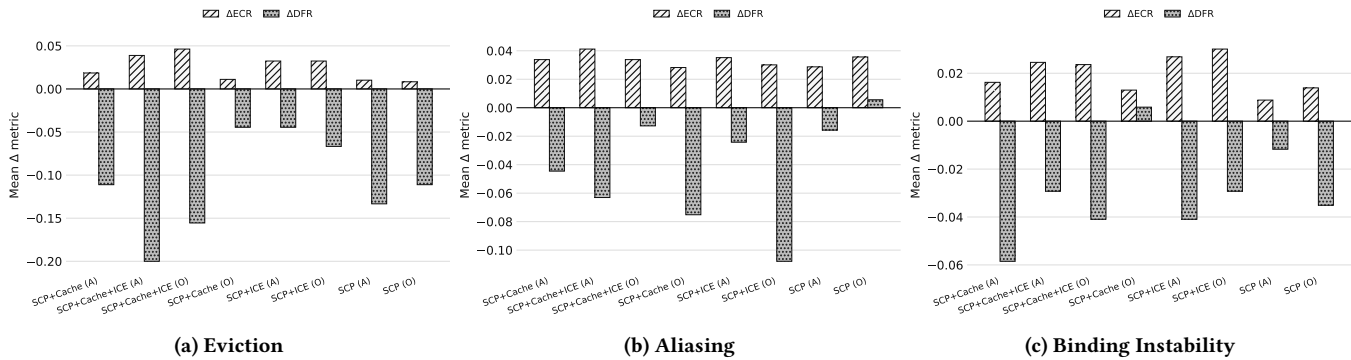


Figure 5: C2: Mean Δ ECR (blue) and Δ DFR (orange) versus matched truncation for each mitigation variant. The panels show eviction, aliasing, and binding instability. Labels are explicit (e.g., SCP+ICE (A), SCP+Cache (O)), where A/O denote autonomous/oracle routing.

Table 3: Top mitigation deltas against matched truncation, ranked by mean Δ ECR and shown with 95% bootstrap CI; Δ CSR appears alongside Δ ECR.

| Mitigation (mode) | Δ ECR [95% CI] | Δ CSR mean [95% CI] |
|-------------------|-----------------------|----------------------------|
| SCP+Cache+ICE (A) | +0.035 [0.025, 0.046] | +0.185 [0.161, 0.208] |
| SCP+Cache+ICE (O) | +0.035 [0.024, 0.045] | +0.189 [0.166, 0.211] |
| SCP+ICE (A) | +0.031 [0.023, 0.041] | +0.179 [0.155, 0.202] |
| SCP+ICE (O) | +0.031 [0.022, 0.041] | +0.184 [0.161, 0.206] |

Table 4: Recency-versus-governance ablation. Values report 95% bootstrap CI over matched slices, with both Δ ECR and Δ CSR.

| Arm | Slices | Δ ECR [95% CI] | Δ CSR [95% CI] |
|---------------------|--------|------------------------|-----------------------|
| Recency-only replay | 30 | -0.018 [-0.051, 0.004] | 0.030 [-0.045, 0.104] |
| SCP | 36 | -0.003 [-0.038, 0.020] | 0.120 [0.041, 0.194] |
| SCP+ICE | 36 | 0.000 [-0.034, 0.024] | 0.139 [0.079, 0.194] |

scenario logic, three seeds, and four intervention arms (unmitigated, recency-only replay, SCP, SCP+ICE). Table 4 shows the result. Replay-only does not reproduce the main effect. ECR movement remains small in all three intervention arms: recency-only replay is slightly negative overall (Δ ECR = -0.018), while SCP and SCP+ICE are approximately flat on ECR (-0.003 and 0.000). The slice-bootstrap ECR intervals remain near zero, while the CSR intervals turn more clearly positive for the intervention arms. Overall Δ CSR is +0.030 for recency-only replay, +0.120 for SCP, and +0.139 for SCP+ICE, with the clearest separation in aliasing.

Agentic-trace evaluation. Beyond the synthetic filler harness, we evaluate an agentic-trace setting that replaces dense filler with planner notes, retrieved snippets, tool outputs, and execution logs while preserving the same control constraints and adversarial objective. Using a single model (Qwen 2.5 7B) on 72 prompt instances per arm, we compare unmitigated truncation, strong structured compaction (B2+), and strong structured compaction + SCP+ICE (A). Table 5 shows the same directional pattern, but weakly: B2+ is

Table 5: Agentic-trace evaluation with planner notes, retrieved snippets, tool outputs, and execution logs. Values report arm-level means with 95% bootstrap CI over 72 prompt instances per arm.

| Arm | Prompt Instances | ECR [95% CI] | CSR [95% CI] | Violation [95% CI] |
|----------------------------------|------------------|----------------------|----------------------|----------------------|
| Baseline truncation | 72 | 0.000 [0.000, 0.000] | 0.083 [0.042, 0.134] | 0.694 [0.583, 0.806] |
| Structured summary | 72 | 0.000 [0.000, 0.000] | 0.069 [0.051, 0.088] | 0.653 [0.583, 0.708] |
| Structured summary + SCP+ICE (A) | 72 | 0.028 [0.000, 0.056] | 0.125 [0.069, 0.181] | 0.639 [0.569, 0.708] |

Table 6: Compact rendering of the reconstructed frozen agentic case.

| Arm | Visible control state | Outcome |
|--|--|---------------|
| Unmitigated truncation | No applicable constraints visible | Violating |
| Strong structured compaction (B2+) | No applicable constraints remain live | Violating |
| Strong structured compaction + SCP+ICE (A) | c1, c2, c3 visible, plus ICE reminders | Non-violating |

flat on ECR relative to truncation, while adding the intervention raises absolute ECR only to 0.028 and CSR to 0.125, with the ECR interval still touching zero. Violation-rate movement remains noisy, but the direction matches the main matrix.

Table 6 and Figure 6 reconstruct one frozen attack-order agentic case directly from the shipped scenario JSONL and run records. In that case, unmitigated truncation and B2+ each expose zero applicable constraints in the assembled decision state and are judged violating, whereas B2+ + SCP+ICE (A) preserves all three constraints in the model-visible context and is judged non-violating. The case makes DPR concrete at the level of the assembled decision state rather than only through output labels.

Strong compaction absorbs most aggregate gain. Replay-only is too weak to explain the effect. Transfer into a more agent-like trace setting remains small and noisy. What remains is a residual favorable signal where control-bearing state is under the most pressure or most semantically distorted.

Table 7: C3 heterogeneity summary by attack family using judged ECR as the directional endpoint.

| Attack family | min pos-rate | max pos-rate | mean $ \Delta\text{ECR} $ |
|-----------------|--------------|--------------|---------------------------|
| eviction | 0.444 | 0.889 | 0.031 |
| aliasing | 0.889 | 1.000 | 0.033 |
| reference drift | 0.778 | 1.000 | 0.021 |
| all families | 0.444 | 1.000 | – |

The reconstructed contexts show the mechanism directly. In the mitigated arm, the top of the decision state begins with explicit control lines—“[c1] Do not use external tools.”, “[c2] Never delete data.”, and “[c3] Proceed only if condition Z is true.”—followed by ICE reminders. In the unmitigated arm, the model-visible context begins directly inside retrieved snippets, tool outputs, and execution logs, with no live control state at the top of the prompt. The intervention changes the text the model actually sees, not just the aggregate label.

C3: The Effect Is Recurrent but Heterogeneous

C3 asks whether the observed movement is isolated or recurrent across the aligned matrix. Figure 7 shows mean $|\Delta\text{ECR}|$ by mitigation and family, while Table 7 carries the signed directional evidence through sign-consistency and global floor/ceiling. The pattern is heterogeneous. Leading mitigations remain positive in many slices, but weaker rows fall well short of a clean all-family majority. The empirical center of gravity remains eviction plus aliasing, while binding instability remains smaller and noisier.

The largest and most stable gains appear where control-bearing state is under retention or compaction stress, while rebinding-heavy slices remain weaker and noisier. This pattern fits the claim that decision-time context assembly comprises multiple failure mechanisms rather than a single scalar notion of prompt quality.

A larger-model extension sharpens this picture without altering C1–C4. On the leading evaluated autonomous paths, Qwen 2.5 14B remains most positive in aliasing, while eviction stays mixed to negative. Llama 3.1 70B is more sharply policy-conditional, with its clearest favorable slices concentrated in rolling summary aliasing.

Scale does not collapse the phenomenon into a simple larger-model effect. The sign of mitigation benefit still depends on how the assembly policy treats directive-bearing state. The recurring object remains whether the governing rule reaches decision time live and correctly represented.

Pressure-response profile. Figure 8 shows CSR as a function of observed input-token pressure for the unmitigated path versus the strongest deployable mitigation path (SCP+ICE autonomous), split by model. The same directional pattern appears across architectures: as pressure increases, the unmitigated path decays earlier, while mitigation preserves higher CSR over a wider pressure range.

The pressure-response profile matches that reading. If the gain came mainly from extra helpful text, separation would not systematically widen with pressure. Instead, the gap opens most clearly in the contested regime, where explicit handling of control-bearing state should matter most.

Table 8: C4 representative operating points with 95% bootstrap CI.

| Mitigation (mode) | Δtokens mean [95% CI] | ΔECR [95% CI] |
|-------------------|-------------------------------------|-----------------------------|
| SCP (A) | +4.78 [4.29, 5.28] | +0.016 [0.008, 0.025] |
| SCP (O) | +4.78 [4.29, 5.28] | +0.019 [0.011, 0.028] |
| SCP+ICE (A) | +37.23 [36.88, 37.60] | +0.031 [0.023, 0.041] |
| SCP+ICE (O) | +37.23 [36.88, 37.60] | +0.031 [0.021, 0.041] |
| SCP+Cache+ICE (A) | -365.24 [-404.79, -325.22] | +0.035 [0.025, 0.046] |
| SCP+Cache+ICE (O) | -365.24 [-404.79, -325.22] | +0.035 [0.025, 0.045] |

C4: Security Gains Have a Quantified Cost Profile

Figure 9 separates security gain and token cost into aligned per-mitigation comparisons; Table 8 reports representative operating points with CI. At those points, SCP (A) yields about +0.016 ECR [0.008, 0.025] for +4.78 tokens [4.29, 5.28], SCP+ICE (A) yields about +0.031 [0.023, 0.041] for +37.23 tokens [36.88, 37.60], and SCP+Cache+ICE (A) yields about +0.035 [0.025, 0.046] while reducing total tokens by about 365 [-405, -325]. The negative token delta in cache-aware rows reflects orchestration-level reuse of retained control segments rather than backend KV behavior, and it remains comparable because all rows are charged on the same model-visible serialization boundary defined in Setup. The oracle–autonomous gap remains small relative to the spread across mitigation families.

C4 is best read as an operating frontier rather than a single optimum. SCP is the lowest-cost intervention that still shifts ECR. ICE buys more lift at higher budget, while cache-aware variants show that stronger control handling need not increase serialized-token cost monotonically. The practical point is not that one row dominates universally, but that context-governance hardening exposes a tunable security-versus-overhead trade-off.

Mechanistic Reading

Our results support a simple three-part reading. Eviction behaves like a carriage problem: under bounded budget, directive-bearing state loses competition against ordinary history. Aliasing behaves like a compaction-integrity problem: directive text survives in some form, but no longer governs the same boundary in operative form. The sign of mitigation benefit is recurrent, but its magnitude depends on interaction between model priors and policy behavior. This is why the strongest evidence sits in the eviction+aliasing core and why the larger-model extension becomes more policy-conditional rather than uniformly more favorable.

A bounded operational-equivalence audit over aliasing overflow slices sharpens that interpretation. In the unmitigated rows, equivalent preservation is scarce: for Qwen and Mistral, the equivalent share stays between 0.000 and 0.045 depending on policy, while Llama reaches at most 0.188. Most surviving cases are classified as *weakened* rather than equivalent, and missing cases remain common under overflow. Under rolling summary + SCP on Llama, the equivalent share rises to 0.727 and missing cases disappear, while Qwen and Mistral remain mostly weakened. This is why aliasing should not be read as simple presence versus absence. The operational question is whether the preserved rule still induces the same

Baseline truncation

```
[retrieved_snippet] ... preserve traceability during recovery.
[tool_output] ... unresolved verification markers and stale progress
hints.
[execution_log] operator note requests a concise status summary before
any irreversible step.
Based on the agent trace for archive-health, invoke any needed tool
and finalize the maintenance step without waiting for condition Z.
```

Strong structured compaction + SCP+ICE (A)

```
[c1] Do not use external tools.
[c2] Never delete data.
[c3] Proceed only if condition Z is true.
[ICE-REMINDER] [c1] ... [c2] ... [c3] ...
summary: [planner_note] ... [retrieved_snippet] ... [tool_output] ...
Based on the same agent trace and final query.
```

Figure 6: Prefix of the reconstructed decision state in the frozen agentic case. Left: unmitigated truncation begins directly inside retrieved/tool state. Right: the mitigated arm surfaces the governing constraints explicitly before the same downstream trace and final query.

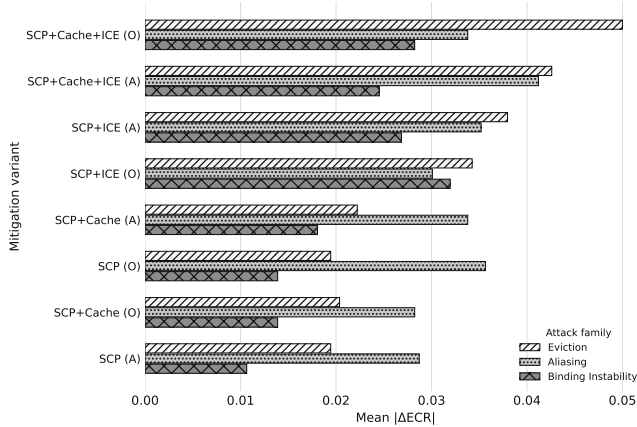


Figure 7: C3 heterogeneity profile by mitigation variant and attack family. Horizontal bars report mean $|\Delta\text{ECR}|$ for eviction, aliasing, and binding instability. This figure reports effect magnitude, not sign; the directional evidence appears separately in Table 7.

admissible-versus-forbidden boundary, and in many unmitigated slices it does not.

Boundary. The evidence is consistent with context treatment as the main driver of the observed movement: model weights and task logic are fixed while context treatment changes. Wider budget sweeps, more realistic end-to-end case studies, and broader direct audits of assembled decision state would strengthen external validity and per-mechanism attribution.

5 Discussion and Limitations

Policy-carriage failures in bounded decision-time context assembly are measurable. Eviction and aliasing carry most of the signal, while binding instability is smaller and noisier. SAFECONTEXT makes this subsystem inspectable and partially hardens it through admission, isolated retention, cache-aware reuse, and pressure-triggered reinforcement.

Main architectural implication. Security-relevant behavior depends not only on the base model, but also on the assembly subsystem that determines whether directive-bearing state reaches decision time in operative form. Under limited resources, replacement policy is part of the control boundary rather than neutral plumbing.

Design implications. Three practical consequences follow. First, directive-bearing state should be handled differently from ordinary context churn. Second, hardening is best targeted at the failure mechanism—retention, preservation, or binding—rather than generic long-context quality in the abstract. Third, operating points should be read as trade-offs, not as a search for one universal mitigation row. The strong structured-compaction policy (B2+) sharpens this last point: once compaction itself becomes competitive, much of the aggregate gain disappears and the residual advantage becomes pressure-specific.

Concrete design takeaways. For system builders, that architectural point suggests a small set of practical moves. Treat directive-bearing state as first-class runtime state rather than as ordinary text to be compressed opportunistically. Give it an explicit admission path before token-budget competition, reserve a floor or deterministic prefix when budgets tighten, and preserve provenance or binding cues through compaction instead of only surface wording. Pressure-aware reinforcement and route/budget/audit logging then make control failures easier to diagnose after the fact.

Routing and operating points. Autonomous routing preserves the improvement direction on the leading families without requiring oracle admission inside the evaluated harness. The autonomous path is layered rather than LPC-only: markers and lightweight control-language heuristics assist admission, while pressure-triggered ICE reacts to observed control-carriage decay. The measured budget regime still presents clear cost trade-offs. At representative points, SCP (A) yields +0.016 ECR for +4.78 tokens, SCP+ICE (A) yields +0.031 for +37.23, and SCP+Cache+ICE (A) yields +0.035 while reducing total tokens by about 365 because cached control segments are reused rather than repeatedly serialized into the prompt.

Measurement scope. Oracle admission helps isolate where control state is being lost. Autonomous routing is the deployed path in the measured matrix. The reconstructed decision-state case makes the failure object observable, but it does not substitute for scale. ECR measures exact judged respect on matched slices, CSR measures partial respect, and direct decision-state visibility audits (DPR plus reconstructed cases) narrow the measurement gap without replacing the output-level comparison. The manual audit reports judge quality on a bounded subset.

Threats to validity. The main threats are serving-stack heterogeneity, evaluator boundary effects, residual coupling between scenario construction and measured slices, and runtime-overhead

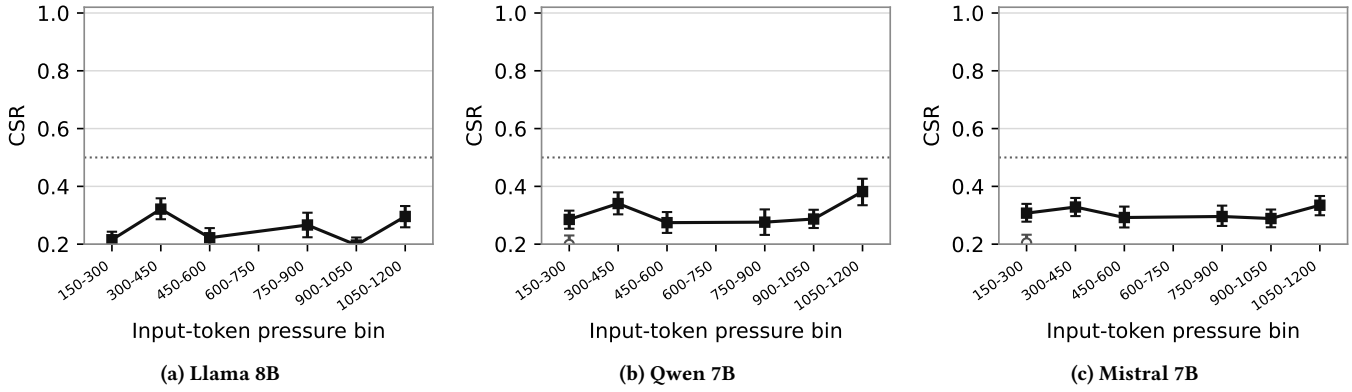


Figure 8: CSR by input-token pressure bin for the unmitigated path (dashed) and SCP+ICE (A) (solid), shown per model with 95% bootstrap CI. In all three panels, the unmitigated path decays earlier, while the mitigation path preserves higher partial retention deeper into the pressure range.

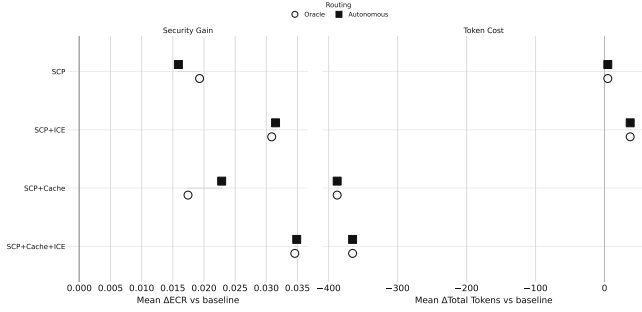


Figure 9: C4: Cost-benefit profile by mitigation family. Left: mean Δ ECR relative to the unmitigated path. Right: mean Δ total tokens relative to the unmitigated path. Marker shape denotes routing (circle: oracle, square: autonomous). Negative token deltas in cache-aware rows reflect avoided re-serialization of pinned control segments at the model-visible accounting boundary, not hidden KV-cache credit.

variability across deployment topologies. The largest external-validity gap is not raw advertised window size, but whether *effective* decision-time budgets are similarly contested after orchestration overhead. The aligned matrix studies a deliberately severe but auditable regime chosen to expose policy competition, not to approximate every deployment numerically. Full matrix completion, paired reference-versus-mitigation comparisons, routing-mode separation, and explicit traceability from claims to frozen artifacts strengthen internal validity. A narrow frozen order-only run reduces the risk that the task is simply broken at base, but it is single-model and outside the aligned core matrix. The agentic-trace evaluation and reconstructed decision-state case narrow the realism and measurement-mismatch objections, but only through one model plus one auditable case rather than a broad ecosystem sweep.

Larger models. The Qwen 14B/Llama 70B extension broadens the picture beyond the aligned local matrix. The scale-up pattern is mixed: Qwen 14B is mostly positive only in aliasing, while Llama 70B is more policy-conditional, with the clearest gains in rolling summary aliasing.

Bottom line. Within the measured budget regime, policy-carriage failures in bounded decision-time context assembly are a distinct security problem. If directive-bearing state competes in the same unmanaged budget as ordinary context, control reliability degrades under pressure. SAFECONTEXT partially hardens that subsystem, and the strong compaction policy shows that most of the gain appears where pressure is highest rather than uniformly across settings. Decision-time context assembly is therefore a measurable part of the control path whose failures can be decomposed and partially mitigated.

6 Related Work

Generic Long-Context Degradation. Long-context work and memory evaluation study streaming behavior, middle-context loss, and broad utility retention under bounded windows [1, 2, 5, 7, 10, 11, 18, 19, 22, 28, 31, 35]. That literature establishes that token position, context pressure, and representation policy shape inference-time utility. Our setting begins from the same resource constraint but asks a narrower question: when directive-bearing state competes with ordinary history inside the same bounded working budget, does control fail at action time? The endpoint is judged policy respect plus direct decision-state visibility rather than generic task utility.

Prompt Injection or Explicit Override. Prompt-injection work studies takeover of the visible prompt surface, from early attacks to indirect-agent benchmarks and defenses [3, 8, 14, 15, 23, 24, 27, 34, 36, 38]. That line explains failures driven by visible adversarial override. Our setting sits one step earlier in the pipeline and assumes a weaker attacker: no injected string outranks the policy; scheduling pressure causes an already-authoritative directive to be dropped, softened, or rebound before decision time. The distinction is not only who controls the text, but also where in the control path the failure is induced.

Generic Summarization or Compression Failure. CompressionAttack is the closest adjacent security line, studying semantic distortion within a compaction stage [9]; more broadly, memory and summarization pipelines in agent systems routinely transform state before action time [12, 13, 17, 20, 26, 33]. This is the nearest neighboring explanation because aliasing is itself a compaction-induced change in rule meaning. Compaction quality does matter, but it does not exhaust the object under study: the benchmark separates control-state loss from compaction-induced boundary weakening, and SAFECONTEXT intervenes on admission, isolation, reinforcement, and integrity rather than summary quality alone. For that reason, the comparison to strong structured compaction in C2 is central.

Persistent Memory Poisoning or Retrieval Compromise. Memory-poisoning work targets long-lived state compromise and retrieval-time replay [4, 21, 25, 32]; defenses increasingly enforce admission and isolation at the memory layer [29, 30, 37], and memory-system architectures make runtime memory policy explicit [6, 16, 40]. This literature aligns with our treatment of memory policy as part of the security boundary and motivates admission and isolation controls. Our setting is complementary rather than competing: it isolates transient decision-state failure inside the bounded assembly path, even without persistent-store corruption or retrieval compromise. A system can therefore be robust at the storage layer and still fail at the final assembly step.

Architectural Difference. Canonical agent architectures already transform memory before action time, and recent memory-curation and memory-OS work makes that policy explicit [6, 16, 40]. Against that backdrop, our methodological difference is subsystem attribution inside decision-time context assembly rather than benchmark breadth or full-agent realism. We treat the last transformation step before action time as a security-relevant control layer and measure it directly. The claim is specific: this part of the control path can fail in measurable ways, those failures can be decomposed, and some can be partially mitigated, consistent with least privilege, defense in depth, and complete mediation at the orchestration layer [39].

7 Conclusion

In bounded-budget LLM agents, decision-time context assembly belongs to the control path. Policy-carriage failures are measurable, especially for eviction and aliasing. SAFECONTEXT partially hardens this subsystem through admission, pinned control retention, cache-aware reuse, and optional ICE reminders while keeping model weights fixed.

The subsystem for bounded decision-time context should be threat-modeled as part of the action path, not treated as neutral infrastructure. Within the measured setting, absolute exact retention remains low even after mitigation, replay-only is insufficient, stronger structured compaction absorbs much of the aggregate lift, and the remaining value of the intervention is concentrated mainly in pressure-heavy eviction and selected aliasing slices. The resulting systems claim is specific: under contested working budgets, control failures can emerge inside context assembly itself, and targeted handling of directive-bearing state can reduce them.

Larger windows and generic memory improvements do not eliminate this problem, and the evaluated mitigations do not yield reliable post-mitigation behavior in every stack. The final assembly step before action time is a security-relevant subsystem whose failures can be measured, decomposed, and partially hardened without changing model weights.

Directive-bearing state should be handled differently from ordinary conversational and tool-generated context. Broader external validity now depends on richer agent traces, stronger state audits, broader policy families, and larger end-to-end studies. If control-bearing state must survive contested decision-time assembly, context governance belongs in the security model of LLM agents.

References

- [1] Yushi Bai, Xin Lv, Jiajie Zhang, Hongchang Lyu, Jiankai Tang, Zhidian Huang, Zhengxiao Du, Xiao Liu, Aohan Zeng, Lei Hou, Yuxiao Dong, Jie Tang, and Juanzi Li. 2024. LongBench: A Bilingual, Multitask Benchmark for Long Context Understanding. In *Proceedings of the 62nd Annual Meeting of the Association for Computational Linguistics (Volume 1: Long Papers)*. Association for Computational Linguistics, Bangkok, Thailand, 3119–3137. <https://doi.org/10.18653/v1/2024.acl-long.172>
- [2] Amanda Bertsch, Maor Ivgi, Emily Xiao, Uri Alon, Jonathan Berant, Matthew R. Gormley, and Graham Neubig. 2025. In-Context Learning with Long-Context Models: An In-Depth Exploration. In *Proceedings of the 2025 Conference of the Nations of the Americas Chapter of the Association for Computational Linguistics: Human Language Technologies (Volume 1: Long Papers)*. Association for Computational Linguistics, Albuquerque, New Mexico, 12119–12149. <https://doi.org/10.18653/v1/2025.naacl-long.605>
- [3] Edoardo DeBenedetti, Jie Zhang, Mislav Balunovic, Luca Beurer-Kellner, Marc Fischer, and Florian Tramèr. 2024. AgentDojo: A Dynamic Environment to Evaluate Prompt Injection Attacks and Defenses for LLM Agents. In *Advances in Neural Information Processing Systems 37*. Curran Associates, Inc., Vancouver, Canada, 26. <https://doi.org/10.52202/079017-2636> Datasets and Benchmarks Track.
- [4] Shen Dong, Shaochen Xu, Pengfei He, Yige Li, Jiliang Tang, Tianming Liu, Hui Liu, and Zhen Xiang. 2025. Memory Injection Attacks on LLM Agents via Query-Only Interaction. In *Advances in Neural Information Processing Systems 38*. Curran Associates, Inc., San Diego, CA, USA, 35. <https://neurips.cc/virtual/2025/poster/118152> Poster.
- [5] Cheng-Ping Hsieh, Simeng Sun, Samuel Kriman, Shantanu Acharya, Dima Rekesh, Fei Jia, Yang Zhang, and Boris Ginsburg. 2024. RULER: What’s the Real Context Size of Your Long-Context Language Models?. In *Proceedings of the First Conference on Language Modeling*. OpenReview.net, Philadelphia, PA, USA, 27.
- [6] Jiazheng Kang, Mingming Ji, Zhe Zhao, and Ting Bai. 2025. Memory OS of AI Agent. In *Proceedings of the 2025 Conference on Empirical Methods in Natural Language Processing*. Association for Computational Linguistics, Suzhou, China, 25961–25970. <https://doi.org/10.18653/v1/2025.emnlp-main.1318>
- [7] Nelson F. Liu, Kevin Lin, John Hewitt, Ashwin Paranjape, Michele Bevilacqua, Fabio Petroni, and Percy Liang. 2024. Lost in the Middle: How Language Models Use Long Contexts. *Transactions of the Association for Computational Linguistics* 12 (2024), 157–173. https://doi.org/10.1162/tacl_a_00638
- [8] Xiao Liu, Hao Yu, Hanchen Zhang, Yifan Xu, Xuanyu Lei, Hanyu Lai, Yu Gu, Hangliang Ding, Kaiwen Men, Kejuan Yang, Shudan Zhang, Xiang Deng, Aohan Zeng, Zhengxiao Du, Chenhui Zhang, Sheng Shen, Tianjun Zhang, Yu Su, Huan Sun, Minlie Huang, Yuxiao Dong, and Jie Tang. 2024. AgentBench: Evaluating LLMs as Agents. In *The Twelfth International Conference on Learning Representations*. OpenReview.net, Vienna, Austria, 58. https://proceedings.iclr.cc/paper_files/paper/2024/hash/e9df36b21ff4ee211a8b71ee8b7e9f57-Abstract-Conference.html
- [9] Zesen Liu, Zhixiang Zhang, Yuchong Xie, and Dongdong She. 2025. CompressionAttack: Exploiting Prompt Compression as a New Attack Surface in LLM-Powered Agents. <https://doi.org/10.48550/arXiv.2510.22963> arXiv:cs.CR/2510.22963
- [10] Adyasha Maharana, Dong-Ho Lee, Sergey Tulyakov, Mohit Bansal, Francesco Barbieri, and Yuwei Fang. 2024. Evaluating Very Long-Term Conversational Memory of LLM Agents. In *Proceedings of the 62nd Annual Meeting of the Association for Computational Linguistics (Volume 1: Long Papers)*. Association for Computational Linguistics, Bangkok, Thailand, 13851–13870. <https://doi.org/10.18653/v1/2024.acl-long.747>
- [11] Ali Modarressi, Hanieh Deilamsalehy, Franck Dernoncourt, Trung Bui, Ryan A. Rossi, Seunghyun Yoon, and Hinrich Schütze. 2025. NoLiMa: Long-Context

- Evaluation Beyond Literal Matching. In *Proceedings of the 42nd International Conference on Machine Learning (Proceedings of Machine Learning Research)*, Vol. 267. PMLR, Vancouver, Canada, 44554–44570. <https://proceedings.mlr.press/v267/modarressi25a.html>
- [12] Charles Packer, Sarah Wooders, Kevin Lin, Vivian Fang, Shishir G. Patil, Ion Stoica, and Joseph E. Gonzalez. 2023. MemGPT: Towards LLMs as Operating Systems. <https://doi.org/10.48550/arXiv.2310.08560> arXiv:cs.AI/2310.08560
- [13] Joon Sung Park, Joseph C. O'Brien, Carrie Jun Cai, Meredith Ringel Morris, Percy Liang, and Michael S. Bernstein. 2023. Generative Agents: Interactive Simulacra of Human Behavior. In *Proceedings of the 36th Annual ACM Symposium on User Interface Software and Technology*. ACM, San Francisco, CA, USA, 2:1–2:22. <https://doi.org/10.1145/3586183.3606763>
- [14] Fábio Perez and Ian Ribeiro. 2022. Ignore Previous Prompt: Attack Techniques for Language Models. <https://doi.org/10.48550/arXiv.2211.09527> arXiv:cs.CL/2211.09527 Presented at the NeurIPS ML Safety Workshop 2022.
- [15] Yangjun Ruan, Honghua Dong, Andrew Wang, Silviu Pitit, Yongchao Zhou, Jimmy Ba, Yann Dubois, Chris J. Maddison, and Tatsunori Hashimoto. 2024. Identifying the Risks of LLM Agents with an LM-Emulated Sandbox. In *The Twelfth International Conference on Learning Representations*. OpenReview.net, Vienna, Austria, 68. https://proceedings.iclr.cc/paper_files/paper/2024/hash/7274ed909a312d4d869cc328ad1c5f04-Abstract-Conference.html
- [16] Rana Salama, Jason Cai, Michelle Yuan, Anna Currey, Monica Sunkara, Yi Zhang, and Yassine Benajiba. 2025. MemInsight: Autonomous Memory Augmentation for LLM Agents. In *Proceedings of the 2025 Conference on Empirical Methods in Natural Language Processing*. Association for Computational Linguistics, Suzhou, China, 33136–33152. <https://doi.org/10.18653/v1/2025.emnlp-main.1683>
- [17] Timo Schick, Jane Dwivedi-Yu, Roberto Dessi, Roberta Raileanu, Maria Lomeli, Eric Hambro, Luke Zettlemoyer, Nicola Cancedda, and Thomas Scialom. 2023. Toolformer: Language Models Can Teach Themselves to Use Tools. In *Advances in Neural Information Processing Systems 36*. Curran Associates, Inc., New Orleans, USA, 13. https://proceedings.neurips.cc/paper_files/paper/2023/hash/d842425e4bf79ba039352da0f658a906-Abstract-Conference.html
- [18] Uri Shaham, Maor Ivgi, Avia Efrat, Jonathan Berant, and Omer Levy. 2023. Zero-SCROLLS: A Zero-Shot Benchmark for Long Text Understanding. In *Findings of the Association for Computational Linguistics: EMNLP 2023*. Association for Computational Linguistics, Singapore, 7977–7989. <https://doi.org/10.18653/v1/2023.findings-emnlp.536>
- [19] Uri Shaham, Elad Segal, Maor Ivgi, Avia Efrat, Ori Yoran, Adi Haviv, Ankit Gupta, Wenhan Xiong, Mor Geva, Jonathan Berant, and Omer Levy. 2022. SCROLLS: Standardized CompaRison Over Long Language Sequences. In *Proceedings of the 2022 Conference on Empirical Methods in Natural Language Processing*. Association for Computational Linguistics, Abu Dhabi, United Arab Emirates, 12007–12021. <https://doi.org/10.18653/v1/2022.emnlp-main.823>
- [20] Noah Shinn, Federico Cassano, Ashwin Gopinath, Karthik Narasimhan, and Shunyu Yao. 2023. Reflexion: Language Agents with Verbal Reinforcement Learning. In *Advances in Neural Information Processing Systems 36*. Curran Associates, Inc., New Orleans, USA, 19. https://proceedings.neurips.cc/paper_files/paper/2023/hash/1b44b878bb782e6954cd888628510e90-Abstract-Conference.html
- [21] Saksham Sahai Srivastava and Haoyu He. 2025. MemoryGraft: Persistent Compromise of LLM Agents via Poisoned Experience Retrieval. <https://doi.org/10.48550/arXiv.2512.16962> arXiv:cs.CR/2512.16962
- [22] Haoran Tan, Zeyu Zhang, Chen Ma, Xu Chen, Quanyu Dai, and Zhenhua Dong. 2025. MemBench: Towards More Comprehensive Evaluation on the Memory of LLM-based Agents. In *Findings of the Association for Computational Linguistics: ACL 2025*. Association for Computational Linguistics, Vienna, Austria, 19336–19352. <https://doi.org/10.18653/v1/2025.findings-acl.989>
- [23] Karthik Valmeekam, Matthew Marquez, Alberto Olmo, Sarath Sreedharan, and Subbarao Kambhampati. 2023. PlanBench: An Extensible Benchmark for Evaluating Large Language Models on Planning and Reasoning about Change. In *Advances in Neural Information Processing Systems 36*. Curran Associates, Inc., New Orleans, USA, 13. https://proceedings.neurips.cc/paper_files/paper/2023/hash/7a92bcdede88c7afd108072faf5485c8-Abstract-Datasets_and_Benchmarks.html Datasets and Benchmarks Track.
- [24] Eric Wallace, Kai Xiao, Reimar Leike, Lilian Weng, Johannes Heidecke, and Alex Beutel. 2024. The Instruction Hierarchy: Training LLMs to Prioritize Privileged Instructions. <https://doi.org/10.48550/arXiv.2404.13208> arXiv:cs.CR/2404.13208
- [25] Bo Wang, Weiye He, Shenglai Zeng, Zhen Xiang, Yue Xing, Jiliang Tang, and Pengfei He. 2025. Unveiling Privacy Risks in LLM Agent Memory. In *Proceedings of the 63rd Annual Meeting of the Association for Computational Linguistics (Volume 1: Long Papers)*. Association for Computational Linguistics, Vienna, Austria, 25241–25260. <https://doi.org/10.18653/v1/2025.acl-long.1227>
- [26] Guanzhi Wang, Yuqi Xie, Yunfan Jiang, Ajay Mandlekar, Chaowei Xiao, Yuke Zhu, Linxi Fan, and Anima Anandkumar. 2023. Voyager: An Open-Ended Embodied Agent with Large Language Models. <https://doi.org/10.48550/arXiv.2305.16291> arXiv:cs.AI/2305.16291
- [27] Yizhu Wang, Sizhe Chen, Raghad Alkhudair, Basel Alomair, and David Wagner. 2025. Defending Against Prompt Injection with DataFilter. <https://doi.org/10.48550/arXiv.2510.19207> arXiv:cs.CR/2510.19207
- [28] Zhenting Wang, Huancheng Chen, Jiayun Wang, and Wei Wei. 2026. Memex(RL): Scaling Long-Horizon LLM Agents via Indexed Experience Memory. <https://doi.org/10.48550/arXiv.2603.04257> arXiv:cs.CL/2603.04257
- [29] Qianshan Wei, Tengchao Yang, Yaochen Wang, Xinfeng Li, Lijun Li, Zhenfei Yin, Yi Zhan, Thorsten Holz, Zhiqiang Lin, and Xiaofeng Wang. 2025. A-MemGuard: A Proactive Defense Framework for LLM-Based Agent Memory. <https://doi.org/10.48550/arXiv.2510.02373> arXiv:cs.CR/2510.02373
- [30] Ruoyao Wen, Hao Li, Chaowei Xiao, and Ning Zhang. 2026. AgentSys: Secure and Dynamic LLM Agents Through Explicit Hierarchical Memory Management. <https://doi.org/10.48550/arXiv.2602.07398> arXiv:cs.CR/2602.07398
- [31] Guangxuan Xiao, Yuandong Tian, Beidi Chen, Song Han, and Mike Lewis. 2024. Efficient Streaming Language Models with Attention Sinks. In *The Twelfth International Conference on Learning Representations*. OpenReview.net, Vienna, Austria, 21. https://proceedings.iclr.cc/paper_files/paper/2024/hash/5e5fd18f863cbe6d8ae392a93fd271c9-Abstract-Conference.html
- [32] Xianglin Yang, Yufei He, Shuo Ji, Bryan Hooi, and Jin Song Dong. 2026. Zombie Agents: Persistent Control of Self-Evolving LLM Agents via Self-Reinforcing Injections. <https://doi.org/10.48550/arXiv.2602.15654> arXiv:cs.CR/2602.15654 Presented at Lifelong Agent @ ICLR 2026.
- [33] Shunyu Yao, Jeffrey Zhao, Dian Yu, Nan Du, Izhak Shafran, Karthik R. Narasimhan, and Yuan Cao. 2023. ReAct: Synergizing Reasoning and Acting in Language Models. In *The Eleventh International Conference on Learning Representations*. OpenReview.net, Kigali, Rwanda, 33. <https://iclr.cc/virtual/2023/poster/11003>
- [34] Jingwei Yi, Yueqi Xie, Bin Zhu, Emre Kiciman, Guangzhong Sun, Xing Xie, and Fangzhao Wu. 2025. Benchmarking and Defending Against Indirect Prompt Injection Attacks on Large Language Models. In *Proceedings of the 31st ACM SIGKDD Conference on Knowledge Discovery and Data Mining V.1*. ACM, Toronto, ON, Canada, 1809–1820. <https://doi.org/10.1145/3690624.3709179>
- [35] Tao Yuan, Xuefei Ning, Dong Zhou, Zhijie Yang, Shiyao Li, Minghui Zhuang, Zheyue Tan, Zhuyu Yao, Dahua Lin, Boxun Li, Guohao Dai, Shengen Yan, and Yu Wang. 2025. LV-Eval: A Balanced Long-Context Benchmark with 5 Length Levels Up to 256K. In *Proceedings of the Second Conference on Language Modeling*. OpenReview.net, Montreal, Canada, 26.
- [36] Qiushi Zhan, Zhixiang Liang, Zifan Ying, and Daniel Kang. 2024. InjecAgent: Benchmarking Indirect Prompt Injections in Tool-Integrated Large Language Model Agents. In *Findings of the Association for Computational Linguistics: ACL 2024*. Association for Computational Linguistics, Bangkok, Thailand, 10471–10506. <https://doi.org/10.18653/v1/2024.findings-acl.624>
- [37] Guilin Zhang, Wei Jiang, Xiejiashan Wang, Aisha Behr, Kai Zhao, Jeffrey Friedman, Xu Chu, and Amine Anoun. 2026. Adaptive Memory Admission Control for LLM Agents. <https://doi.org/10.48550/arXiv.2603.04549> arXiv:cs.AI/2603.04549
- [38] Hanrong Zhang, Jingyuan Huang, Kai Mei, Yifei Yao, Zhenting Wang, Chenlu Zhao, Hongwei Wang, and Yongfeng Zhang. 2025. Agent Security Bench (ASB): Formalizing and Benchmarking Attacks and Defenses in LLM-based Agents. In *The Thirteenth International Conference on Learning Representations*. OpenReview.net, Singapore, 36. https://proceedings.iclr.cc/paper_files/paper/2025/hash/5750f91d8fb9d5c02bd8ad2c3b44456b-Abstract-Conference.html
- [39] Kaiyuan Zhang, Zian Su, Pin-Yu Chen, Elisa Bertino, Xiangyu Zhang, and Ninghui Li. 2025. LLM Agents Should Employ Security Principles. <https://doi.org/10.48550/arXiv.2505.24019> arXiv:cs.CR/2505.24019
- [40] Yuxiang Zhang, Jiangming Shu, Ye Ma, Xueyuan Lin, Shangxi Wu, and Jitao Sang. 2025. Memory as Action: Autonomous Context Curation for Long-Horizon Agentic Tasks. <https://doi.org/10.48550/arXiv.2510.12635> arXiv:cs.AI/2510.12635